Production Engineering (2021) 15:863–871
https://doi.org/10.1007/s11740-021-01066-y

PRODUCTION PROCESS

Path velocity planning for a forming process of fiber-reinforced thermoplastic with six degree of freedom

Birk Wonnenberg[1] · **Klaus Dröder**[1]

Received: 10 February 2021 / Accepted: 17 June 2021 / Published online: 2 July 2021

Abstract
By punch trajectory planning for a multi-axis forming press, it is possible to affect the local material properties in the workpiece. A multi-axis forming process can influence the material flow and thus the material properties via the punch path. During multi-axis forming processes, the velocity on a defined punch path affects the heat transfer between the punch and the forming material. An example for such forming materials is glass mat thermoplastics (GMT). Multi-axis forming can form these materials in a molten state. The materials cool down during forming due to contact-induced heat transfer between material and punch. The contact zone varies during the process and depends on the punch path. The punch velocity, however, influences the duration of the contact. In order to plan the punch velocity for required part properties, this paper presents an analytical model. The model bases on the geometrical description of the contact zone and gives different velocity profiles, which are tested in experiments. Finally, the paper discusses the analytical model, the velocity profiles and the requirements for the press.

Keywords Forming · Tool path · Temperature · Modelling · Process control

1 Introduction

In forming and pressing processes, the tool trajectory is often one-, two- or three-dimensional. More dimensions allow complex trajectories to achieve a higher production flexibility [1]. This paper presents a process called multi-axis forming. Multi-axis forming ranges between forming with a linear tool movement, for example compression molding [2], and forming with a complex tool movement, for example incremental sheet forming [3]. Unlike compression molding, the punch movement is not limited to a linear translation and differs from incremental sheet forming by its broader contact area and workpiece-specific tool shape.

In multi-axis forming, the punch movement can follow a trajectory, for example a superposition of rotation and translation. Trajectories are a combination of path and velocity [4]. The punch trajectory influences the local material properties. While the punch path defines the workpiece geometry and the direction of the material flow, the punch velocity defines for example the cooling of warm forming material. As forming material, this study uses fiber-reinforced thermoplastic.

The benefit from multi-axis forming process is the ability to adjust the material flow in comparison to a linear pressing movement. This material flow can orientate fibers in load direction and result in a material property influenced by the punch trajectory [5]. Further process potentials are an improved form filling and reduced machine forces through smaller pressing areas. Another use case for the multi-axis forming process can be the reduction of the mechanical complexity of the die. An example is the avoidances of sliders by increasing the tool path complexity. Other papers deal with the tool design for a known part and tool path [6], the tool path influence on the material flow [7, 8] or how the material flow can be measured [9].

The scope of this paper is a description of the contact state in the process and the planning of the tool path velocity. The research goal are suitable velocity profiles for multi-axis forming to process fiber-reinforced thermoplastics. First, this paper describes the forming process and the contact state between tool and forming material, followed by preliminary experiments. Second, this paper presents an analytical model

✉ Birk Wonnenberg
b.wonnenberg@tu-braunschweig.de

[1] Institute of Machine Tools and Production Technology, Technische Universität Braunschweig, Langer Kamp 19b, 38106 Brunswick, Germany

that provides different path velocities. Third, this paper demonstrates and discusses the use of the different path velocities in forming experiments.

2 Multi-axis forming of fiber-reinforced thermoplastics

This paper provides a brief process description, since multi-axis forming is not a common forming process. In multi-axis forming, trajectories with six degrees of freedom enable the manufacturing of complex parts.

The concept of multi-axis forming origins from orbital forming. Han et al. [10–12] use a similar approach to achieve more complex parts. These papers show the manufacturing of non-rotary parts through orbital forging. Han et al. [10–12] give a description of the geometrical relation between path and die for a two dimensional trajectory. However, for cold orbital forging, the path velocity is independent of the heat flow.

Conte et al. [3] show that processing fiber-reinforced thermoplastic at glass transition temperature with incremental sheet forming is feasible. The drawback and starting point for further investigations are springback, cracking and overall part inaccuracy.

Subject of the investigations in this paper is forming of materials such as glass mat thermoplastics (GMT). In [2] the cooling behavior of thermoplastic in manufacturing processes is described. The forming of fiber-reinforced thermoplastics requires a heating phase to melt the matrix material, a forming phase and a cooling phase. The cooling to temperatures well below the melting point must take place while the material is still under pressure to ensure consolidation. The authors in [2, 13] give a description of the material flow of fiber-reinforced thermoplastic and the orientation and segregation of fibers.

Known influences on the part shape in a pressing process are material and tool temperature, insertion position and shape as well as pressure and holding time. These influences lead to shrinkage or warpage through fiber segregation and orientation [14, 15]. The focus of this paper is the influence of the tool velocity, which is an uncommon research topic for a pressing process. The machine is path-controlled and the tool path is given. The pressure is a result of the reaction forces. The start temperatures and the insertion position are constant.

In multi-axis forming processes, the punch forms the fiber-reinforced plastic material in the lower die. The drawing in Fig. 1 gives an overview of the forming process. The flow front of the forming material moves in the same direction as the punch movement. In this process, only a part of the punch is in contact with the forming material. The punch

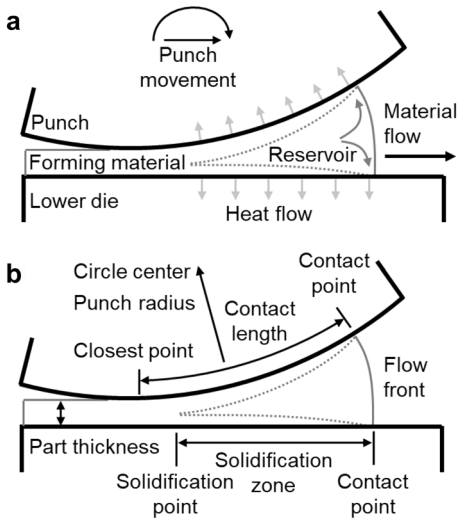

Fig. 1 **a** Multi-axis forming with a static lower die and a punch, which can move in all six dimensions; Heat flow from forming material to die and punch; **b** Geometrical relations

squeezes excessive material ahead. This excessive material is the reservoir of molten material.

The geometry-defining zones of the punch are the current closest points to the final part surface. The solidification line separates the solid material from the zone with molten material. The closest point must be at or in front of the solidification line, as forming of thermoplastics should take place in a molten state. If the complete material is below recrystallization temperature, before the punch finishes forming, the part thickness remains above specification, but if any molten material remain in the part after pressing, a layer of porous material can re-form in the part median plain [16]. Therefore, there is a small process window, in which the forming velocity is optimal.

The examined punch path is a rolling movement over a plain lower die with reduced relative movement between part and punch at the closest points. Figure 1a displays punch, forming material, lower die and material flow as well as the heat flow from forming material to die and the material flow within the reservoir. Figure 1b defines the geometrical relations in the process. The contact point is the first contact between die and forming material. The closest point is the last contact. At the solidification point the upper and lower solid layer of forming material touch. The solidification zone describes the area in which molten material is present between the contact point and the solidification point.

Processes, which are comparable in respect to the cooling behavior, are compression and injection molding. The cooling in compression molding is equivalent to a mechanical static situation with short flow length. In injection molding, the global material flow within a cavity and its flow length

influence the cooling behavior. Both behavior descriptions do not apply to multi-axis forming.

A process with high similarity to multi-axis forming is twin-rolling casting. Numerical investigations [17, 18] give a detailed description of cooling in this process. Both processes, twin-rolling and multi-axis forming, build up a layer of solid thermoplastic in the vicinity to the tool surface. However, twin-rolling is a continuous process, while multi-axis forming is a discontinuous process.

Main factors for the cooling process in multi-axis forming are the initial temperatures, material thickness and the contact time. The cooling at the contact surfaces only affects a thin layer of material due to the low thermal conductivity of the thermoplastic. These factors influence the optimal path velocity profile.

3 Experimental set-up

For the experimental set-up, a six degree of freedom press, for instance a Stewart platform, realizes the multi-axis forming process. The authors in [19, 20] give a description of the press. Figure 2 displays the set-up with six hydraulic cylinders, which are connected to form a parallel kinematic between the frame and a platform that carries the punch.

The forming experiments use glass mat thermoplastics (GMT) S130A248-N1 by Quadrant with a fiber to polypropylene matrix volume ratio of 30%. The melting temperature of the matrix material is 166 °C and the mold shrinkage is 0.2–0.35%. Figure 3 gives a sketch of the tool geometry and the insertion position of the GMT. Before the forming process, the heated GMT has a size of 120 mm by 110 mm by 40 mm (x, y, z) and after the forming, the maximum dimensions are 360 mm by 120 mm and 3 mm. The coordinate system in this tool is set at the surface of a 3 mm part. The

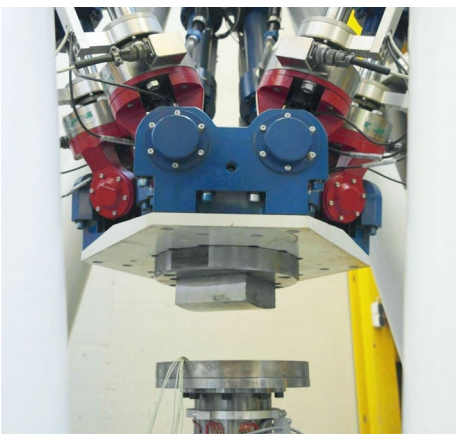

Fig. 2 Experimental press with six hydraulic cylinders

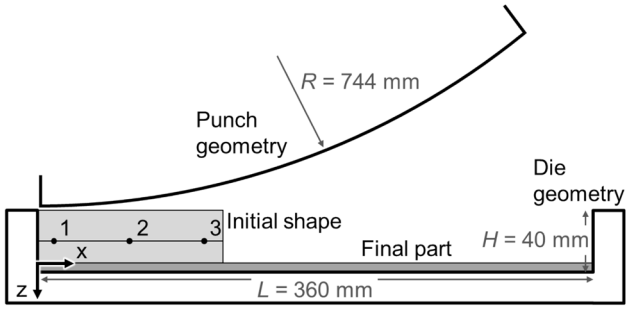

Fig. 3 Cross section of the geometry of the lower die, position of the thermocouples and coordinate system within the lower die; position and shape of the initial GMT in gray (left) (Color figure online)

thermocouple (type K) positions are in the median plane in between two GMT sheets.

A convection oven directly next to the press heats the GMT at 220 °C, after melting the GMT is stacked with thermocouples in between. The heating phase continues until the material core temperature reaches 195 °C. The material is placed in the tool and the tool closes with a linear movement in the z-axis. Beginning from the insertion position, a rolling movement of the punch forms the warm material. Die and punch have a temperature of around 25 °C (room temperature with no heating or cooling system). Measurements of the material thickness in different positions take place after cooling the material down to room temperature.

4 Preliminary tests

Preliminary forming tests show the cooling time for different part thickness. These tests have the same set-up and experimental procedure as described above. The only difference is a flat punch, which moves along the z-axis and holds the lowest position to cool the GMT. Figure 4 displays the

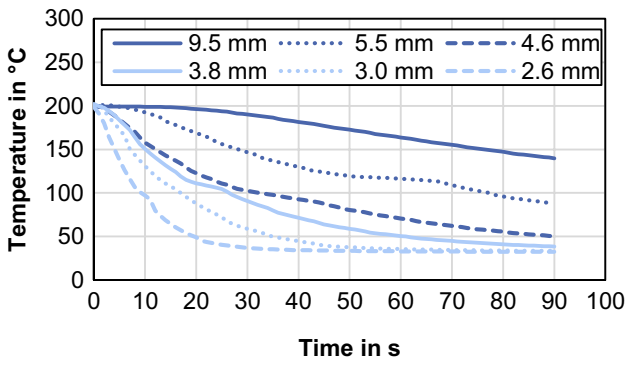

Fig. 4 Temperature at sensor 3 for different thicknesses of a flat punch specimen

averaged measured temperature at sensor 1 to 3 for each part. The standard deviation is 4 °C or lower between each sensor.

Figure 5 displays the heating and cooling curve in a differential scanning calorimetry (DSC) analysis. The recrystallization takes place at 117 °C for a cooling rate of 10 K/s. For a part with 3 mm thickness, the cooling rate is about 7 K/s and it takes 13 s to cool the material to the recrystallization temperature.

The cooling curves show some scatter in this set-up, due to manual operation, local surface cooling and irregular matrix flow. This led to the decision to measure the temperatures only in the preliminary tests but not in the following experiments.

5 Modeling of the cooling behavior

In order to describe the relation between forming velocity, part thickness and part temperature for fiber-reinforced thermoplastic material, this paper presents a phenomenological model. This model considers a section of the material with a constant path velocity.

Figure 6 displays the material thickness (a) and the temperature within the material in the median plane (b) at one location for three path velocities. In this model, the temperature of V1 is apparently too low and solid excess material remains at this position leading to a higher part thickness. The other velocities, V2 and V3, are higher than V1. With these velocities, the excess material is warm and fluent enough resulting in the correct part thickness. The final part thickness remains only correct for parts pressed with V2 velocity. Parts pressed with V3 loft again in the median layer, where the material is too warm to remain consolidated after pressing, resulting in a higher part thickness.

In a first approach, the authors assume a profile with a variable path velocity. The analytical model for planning the path velocity describes the contact state in the forming process. The path velocity is a function of the length of the material in contact divided by a time to cool down

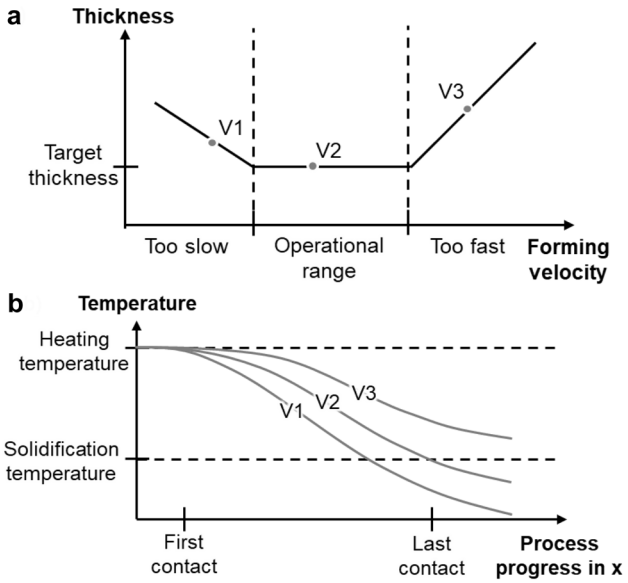

Fig. 6 **a** Illustration of the phenomenological model; **b** Temperature within the part depending on the process progress and the punch velocity

the material. For the calculations, one assumption is that the material surface areas in contact to the die still have the initial heating temperature. This model assumes, that two layers of solid material build up on die and punch surface through cooling. The preliminary tests provide the cooling time for a certain material thickness to solidify. Each layer has to reach half the part thickness and remaining molten material flows out of the pressing gap.

This study analysis a cross section in a rolling punch movement with a flat flow front in any given situation. The current contact area is part of the surface of the remaining reservoir. Figure 7 displays the variables for this model.

The analytical model describes the relation between formed material and remaining reservoir. The volume of the compound is a function of the punch position. The

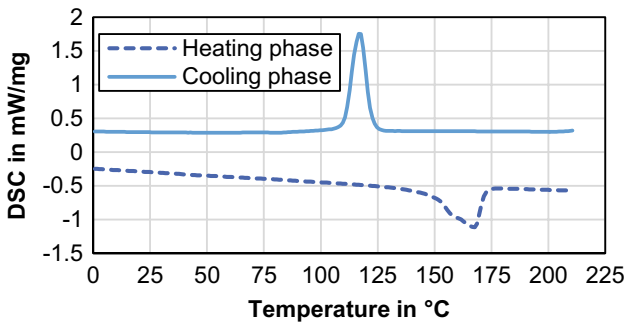

Fig. 5 DSC analysis of the GMT with polypropylene matrix

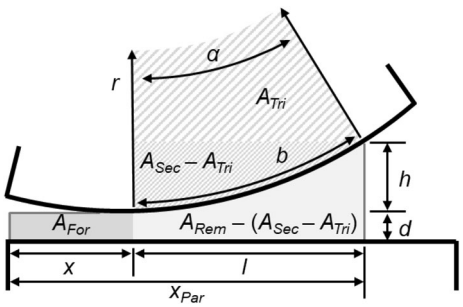

Fig. 7 Variables for the analytical model: formed material length (x), punch radius (r), contact angle (α), material reservoir length (l), contact length (b), part thickness (d), additional flow front height (h)

following equations formulate the analytical model, corresponding to Fig. 7. The constant total material area (A_{Tot}) is the part length (x_{Par}) times the part thickness (d). This is equal to the sum of the formed material (A_{For}), a square area around the remaining material (A_{Rem}) and the triangle in the punch (A_{Tri}), subtracted by a section area of the punch in contact (A_{Sec}):

$$A_{Tot} = A_{For} + A_{Rem} + A_{Tri} - A_{Sec} \tag{1}$$

$$A_{Tot} = x_{Par} * d \tag{2}$$

$$A_{For} = d * x \tag{3}$$

$$A_{Rem} = (h + d) * l \tag{4}$$

$$A_{Tri} = (r - h) * l/2 \tag{5}$$

$$A_{Sec} = r^2 * \alpha/2 \tag{6}$$

$$l = \sin(\alpha) * r \tag{7}$$

$$h = \mathrm{r} - \cos(\alpha) * r \tag{8}$$

Insertion and conversion to the position of the closest point ($x(\alpha)$) result in formula 9:

$$x = (x_{Par} * d - r^2 \sin(\propto) - d\sin(\propto) r$$

$$+\frac{r^2 \sin(\propto)\cos(\propto)}{2}$$

$$+(r^2 * \propto)/2)/d. \tag{9}$$

The contact length (b) is contact angle (α) times punch radius (r). With the closest point ($x(\alpha)$), the contact length ($b(\alpha)$) and a set of parameters $r = 744$ mm, $d = 3$ mm, $x_{Par} = 360$ mm, it is possible to draw a contact length over position curve by using a spreadsheet program like Microsoft Excel, see Fig. 8. Another way to describe the contact state is the sum of tool positions in contact with the material at each point along the x-axis. This sum results in a length hereafter called contact sum. In the calculation of the contact sum, the initial material thickness after heating is 40 mm. With the first movement in z-axis, these 40 mm add to the contact sum of the first 143 mm.

The aim of a model based planning for the path velocity is to generate a velocity profile based on the contact time for each surface point. Two different approaches are possible. With a stepwise movement, the punch stops at a certain point, cools the material down until solidification

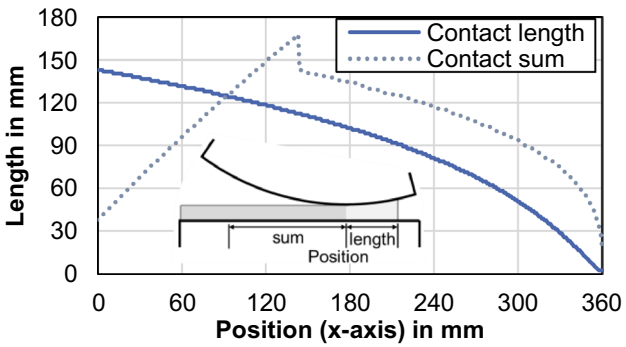

Fig. 8 Contact length and contact sum over closest point position for $r = 744$ mm, $d = 3$ mm and $x_{Par} = 360$ mm

reaches a certain layer thickness and moves to the next position pressing the remaining material out. This cycle of cooling and pressing repeats for the whole part. The step width correlates with the contact length from Fig. 8. The second approach is the use of a variable path velocity. The variable path velocity for each surface point is a function of the contact sum divided by the cooling time.

Figure 9 displays a variable and a stepwise velocity profile as well as a profile for a constant movement. These profiles base on a time frame of 13 s to build up a solid layer of total 3 mm. The variable movement starts in z-axis and continues in x-axis.

The stepwise movement has several positions, each with a cooling time of serval seconds, and an instantanius movement to the next position. The acceleration as well as the velocity of the press restrict this movement, this velocity planning assumes one second for the movement. Along the path, the step size decreases to the end of the forming process. If the flow front is only two millimeters higher than part thickness, the velocity profiles moves directly to the last position and omits the remaining small steps. This procedure simplifies the path planning and shortens the overall process time.

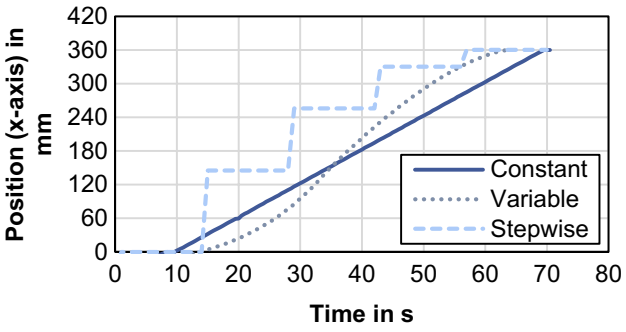

Fig. 9 Punch velocity for constant, variable and stepwise movement with a cooling time of 14 s

6 Experimental results

The validation of the model requires forming tests. The path velocities vary between the highest possible velocity of the press and the slowest possible velocity. The process force restricts the slowest possible velocity, as the material gets too cold to form. A constant velocity profile considers only the closest point and a small area in front of the closest point. It relies on the alternative assumption that the cool down rate depends on the material thickness. This approach is similar to a steady state such as twin-rolling [17, 18].

Figure 10 shows the results as exact process time and the final part thickness along the x-axis. At very short process times, the thickness has a high variety and decreases with longer process times. With a constant forming velocity, it is not possible to achieve a uniform part thickness. The goal for the resulting part thickness is 3 mm. Figure 10 displays part thicknesses of exactly 3 mm in white, higher part thicknesses in red and lower part thicknesses in blue. The color intensity increases in the heat map with higher difference.

Process time in s	Part thickness at position (x-axis) in mm							
	10	50	100	120	150	200	250	300
6.5	4.8	4.9	3.2	3.7	3.9	3.3	3.7	3.0
9	4.4	3.7	3.2	3.4	3.8	3.5	3.3	3.0
11.5	4.8	4.0	3.3	3.2	3.7	3.2	3.0	3.0
14	4.1	3.7	3.2	3.2	3.3	3.1	3.2	3.1
20	4.0	3.6	3.2	3.1	3.6	3.2	3.0	2.8
25	3.7	3.7	3.2	3.1	3.6	3.3	3.4	3.0
31	3.8	3.6	3.2	3.1	3.2	3.2	3.0	
36.5	3.8	3.6	3.3	3.1	3.3	3.0	3.0	2.9
42	3.8	3.6	3.3	3.1	3.4	3.1	3.1	2.9
47.5	3.7	3.4	3.3	3.1	3.3	3.1	3.1	3.0
52	3.6	3.4	3.3	3.2	3.2	3.1	3.1	2.9
58.5	3.7	3.4	3.3	3.2	3.2	3.3	3.0	2.9
70.5	3.5	3.3	3.3	3.3	3.2	3.6	3.6	3.2
81.5	3.4	3.3	3.5	3.6	3.5	3.8	3.9	3.3

Fig. 10 Part thickness as heat map over x-axis and different constant forming velocities

The stepwise forming profile bases on a constant cooling rate independent from the part thickness. The step size varies for each step according to the results in Fig. 9. Table 1 compares the measured and the calculated flow front. Overall, the flow front is not a straight line. The estimation of the flow front by the analytical model falls into the range of measured values. Table 2 displays the input parameters for the stepwise tests with constant step positions and variable cooling times.

Figure 11 displays the thickness over the length of the part. At 10 mm, 50 mm and 200 mm in x-direction the part thickness reaches higher values than average. These values are quite indifferent to longer cooling times. Only at 10 mm occurs a rapid change to smaller values with cooling times higher 9 s.

Figure 12 displays a combination of a constant forming velocity with a stop at start of the rolling movement. At 10 mm x-position, the part thickness after the experiments with a stop is smaller than without. With longer process times, the part thicknesses at 100 mm and 120 mm incline to higher values. The other values are similar to Fig. 10.

7 Discussion

The analytical model bases on part and die geometry. For the example, the estimation of the flow front position is feasible and it is possible to describe the contact length. For complex geometries or punch paths, the model might get

Table 1 Stepwise forming positions; extend of flow front after stepwise forming and the calculated contact length

Step positions in mm			Left	Middle	Right	Calc
0			145	190	178	145
0	145		242	255	261	256
0	145	256	326	344	298	330

Table 2 Position, cooling and process time for the stepwise forming tests

	Step positions in mm					Cooling time in s	Process time in s
E1	0	145	256	330	360	7	40
E2	0	145	256	330	360	9	50
E3	0	145	256	330	360	11	60
E4	0	145	256	330	360	13	70
E5	0	145	256	330	360	15	80

	Part thickness at position (x-axis) in mm							
	10	50	100	120	150	200	250	300
E1	4.4	4.0	3.2	3.1	3.3	3.5	2.7	3.2
E2	4.8	4.3	3.2	3.0	3.8	3.9	2.7	3.3
E3	2.9	4.7	3.4	3.2	3.0	4.2	2.8	3.3
E4	2.5	4.4	3.2	3.0	2.9	4.0	2.7	3.2
E5	3.6	4.7	3.4	3.0	2.8	4.0	2.8	3.4

Fig. 11 Resulting part thickness after stepwise forming as heat map over *x*-axis

Process and cooling time in s		Part thickness at position (x-axis) in mm							
		10	50	100	120	150	200	250	300
31	3	3.7	3.5	3.2	3.0	3.3	3.1	3.1	3.0
36	5	3.5	3.4	3.2	3.1	3.2	3.3	3.0	2.9
42	4	3.7	3.5	3.3	3.1	3.2	3.1	3.1	2.9
42	7	3.6	3.5	3.3	3.2	3.2	3.1	3.1	2.9
42	10	3.2	3.5	3.5	3.4	3.2	3.1	3.1	
42	13	3.0	3.7	3.8	3.6	3.3	3.1	3.1	2.9
47	13	3.0	3.5	3.6	3.5	3.3	3.2	3.3	3.0
52	11	3.2	3.4	3.6	3.5	3.3	3.3	3.1	2.9
59	9	3.3	3.5	3.6	3.5	3.2	3.3	3.1	3.0

Fig. 12 Resulting part thickness for different constant forming velocities including a stop at x = 0 mm as heat map over *x*-axis

too complex. A forming simulation can solve this complex velocity planning.

The authors conducted experiments with a constant path velocity to analyze the process behavior. The part thickness for a constant forming velocity changes gradually depending on the path velocity. The areas in Fig. 13 describe the thickness deviations in Fig. 10. The tolerance for the part thickness is 0 mm to 0.3 mm. The mold shrinkage for 3 mm part thickness is around 0.01 mm and therefore neglected.

In region a, the material thickness is too high but decreases with longer process times, which indicates unfinished consolidation due to too short contact times. The same applies to region b. The analytical model explains the region a and shows that contact times are too short. However, it does not provide an explanation for region b so that more investigations for this area are necessary. In region c, the material thickness increases with the process time, which indicates a material that is too cold for forming. In region d, the measured thickness has a high variety over the whole part length, indicating a thin solid layer after the forming. In region e, the low part thicknesses indicate a lack of material.

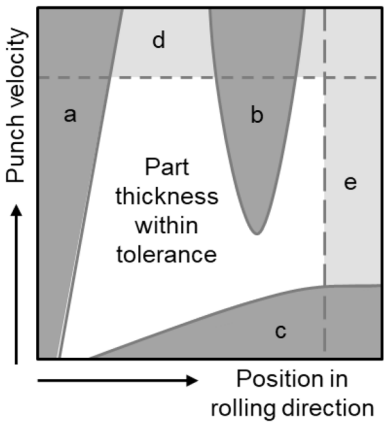

Fig. 13 Areas of the deviation of the part thickness at different constant forming velocities

The stepwise velocity profile has two variables, step width and cooling time. The analytical model describes the step width well enough. The determination of a suitable cooling time was not possible. The cooling time of 13 s has the best forming result and correspond to the estimated cooling time of 13 s for 3 mm, but the cooling behavior depends on the material thickness, Fig. 4. The influence of the material thickness on the cooling behavior is too high for a stepwise approach. Therefore, it is not possible to build up a constant solid layer over the contact length, which results in high varieties of the part thickness. In addition, the very low material thickness at some points indicates an overshoot in the position control of the press due to high dynamics.

A variable velocity profile is suitable to achieve the optimal cooling time for each position. However, even for a simple part geometry as in this study, the shape of this profile is a complex problem. The presented analytical model is not sufficient to solve this problem. This shows that even for simple geometries a forming simulation is necessary. In addition, the position control of the press must have the ability to follow a variable velocity profile.

In nearly all tests, the first 50 mm are difficult to cool down. The experiments show, that a stop at beginning of the rolling phase can solve this problem. Figure 12 shows this improvement.

To summarize the discussion, the best result was achieved with a constant velocity and a stop at the beginning. It is anticipated, that a model based variable punch velocity will provide the best result, with a low velocity at the start, higher velocity in the middle part and a low velocity at the end. The model should integrate the local thickness depended cool down rate of the forming material, since only a contact based model with a constant cool down rate seems not sophisticate enough.

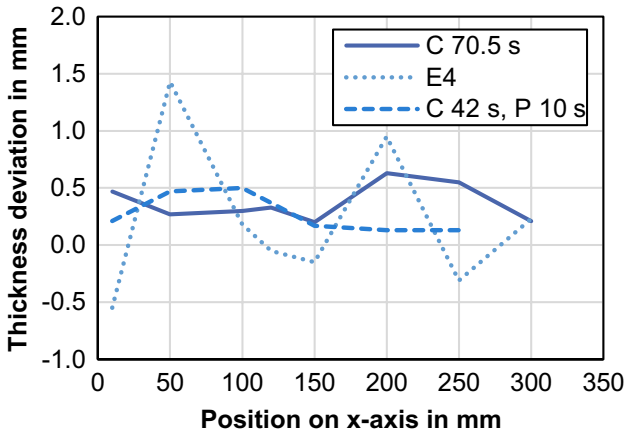

Fig. 14 Comparison of the best forming results: Constant velocity with 70.5 s process time, stepwise profile E7 and constant velocity with 42 s process time and a pause of 10 s

8 Conclusion

This paper introduces multi-axis forming as a process route to form and cool down fiber-reinforced thermoplastics. With punch paths in six dimensions, it is possible to determine the forming and the cooling by the punch trajectory. The punch velocity on this trajectory directly determines the cooling.

To obtain a part in a defined thickness, the progress of the punch and the solidification point separating molten and solid material in the part need to match. This relation allows the determination of suitable path velocity profiles. For planning of these profiles, the study presents a phenomenological model as well as an analytical model. The phenomenological model describes the deviation of the plate thickness depending on the path velocity. While low velocities lead to high process forces and an unfinished forming, higher velocities may lead to an unfinished consolidation and splitting. The analytical model describes the contact area in the forming process that matches well with the test results.

The paper presents experimental results for different velocity profiles, a constant profile and a stepwise profile with high acceleration and velocity. Figure 14 shows a comparison of the best forming results of each velocity profiles with the lowest bias and variance.

The results show, that it is possible to form and cool down the material with a constant velocity profile and a variety of different velocities. The resulting part thickness is not optimal. Throughout all examined velocities, the part thickness is too high at the beginning of the forming process, which indicates an unfinished cooling. An extra stop at the beginning of the forming process is preferable, to address this problem. The tests with this extra stop show overall better results.

The tested stepwise velocity profiles were not suitable for the process. It is possible to model the contact situation for the stepwise profiles, but it is not possible to simplify the cooling time as independent from the local material thickness. The resulting part thickness has a high local variety, which is contrary to the stepwise approach. In addition, the high accelerations and velocities can lead to an overshoot in position control.

Another solution for the punch velocity in multi-axis forming is a variable velocity profile. To gain this velocity profile a forming simulation is inevitable. Future work will concentrate on the flow simulation with a thermal model [15, 21]. By optimizing the final temperature in the part or multiobjectives [22], this simulation can determine the exact parameters of the profile. However, the planning must take the programming and the kinematic of the press into account to realize the velocity profile. This velocity profile can be a table or a function and the machines position control must be able to interpret this velocity profile in an open loop. A closed loop control with process state observer via temperature and pressure sensors is also possible approach.

Before the solution of this complex task in the future, the constant velocity profile with a stop at the beginning is the best option. This study shows that calculation of this profile is feasible with reasonable effort and leads to robust results in practical tests.

Acknowledgements This work was funded by the Deutsche Forschungsgemeinschaft (DFG, German Research Foundation)—318620418. We acknowledge support by the German Research Foundation and the Open Access Publication Funds of Technische Universität Braunschweig. The authors thank Ann-Christin Hesse for assistance during the experiments and the researchers from the Institute of Forming Technology and Machines at Leibniz University Hannover for the good cooperation in the research project.

Funding Open Access funding enabled and organized by Projekt DEAL. This work was funded by the Deutsche Forschungsgemeinschaft (DFG, German Research Foundation)—318620418.

Availability of data and material None.

Code availability None.

Declarations

Conflict of Interest The authors declare that they have no conflict of interest.

References

1. Groche P, Scheitza M, Kraft M et al (2010) Increased total flexibility by 3D Servo Presses. CIRP Ann Manuf Technol 59:267–270. https://doi.org/10.1016/j.cirp.2010.03.013
2. Rosato DV, Rosato DV, Rosato MV (2004) Plastic product material and process selection handbook. Elsevier Advanced Technology, Oxford
3. Conte R, Ambrogio G, Pulice D et al (2017) Incremental sheet forming of a composite made of thermoplastic matrix and glass-fiber reinforcement. Proc Eng 207:819–824. https://doi.org/10.1016/j.proeng.2017.10.835
4. Latombe J-C (1991) Robot motion planning. Springer, Boston
5. Radtke A (2009) Steifigkeitsberechnung von diskontinuierlich faserverstärkten Thermoplasten auf der Basis von Faserorientierungs- und Faserlängenverteilungen. Wissenschaftliche Schriftenreihe des Fraunhofer ICT, vol 45. Fraunhofer IRB-Verl., Stuttgart
6. Wonnenberg B, Müller A, Dröder K (2019) Comparison of design approaches to generate tools for a forming process with a six degree of freedom press. AIP Publishing. https://doi.org/10.1063/1.5112648
7. Dröder K, Behrens B-A, Bohne F et al (2019) Numerical and experimental investigation of thermoplastics in multi-axis forming processes. Procedia CIRP 85:96–101. https://doi.org/10.1016/j.procir.2019.09.024
8. Wonnenberg B, Gabriel F, Dröder K (2021) Directing the material flow and form filling through a multi-axis forming process. ESAFORM 2021. https://doi.org/10.25518/esaform21.4093
9. Wonnenberg B, Dietrich F, Dröder K (2018) In-situ measurement technologies for flow behaviour and contact status of fibre-reinforced thermoplastics during forming with a six degree of freedom press. MATEC Web of Conf 190:7004. https://doi.org/10.1051/matecconf/201819007004
10. Han X, Hua L, Zhuang W et al (2014) Process design and control in cold rotary forging of non-rotary gear parts. J Mater Process Technol 214:2402–2416. https://doi.org/10.1016/j.jmatprotec.2014.05.003
11. Han X, Hu Y, Hua L (2016) Cold orbital forging of gear rack. Int J Mech Sci 117:227–242. https://doi.org/10.1016/j.ijmecsci.2016.09.007
12. Han X, Zhang X, Hua L (2016) Calculation method for rocking die motion track in cold orbital forging. J Manuf Sci Eng 138:14504. https://doi.org/10.1115/1.4030855
13. Ning H, Lu N, Hassen AA et al (2020) A review of long fibre thermoplastic (LFT) composites. Int Mater Rev 65:164–188. https://doi.org/10.1080/09506608.2019.1585004
14. Li X, Gong N, Gao Z et al (2017) Fiber orientation in melt confluent process for reinforced injection molded part. Int J Adv Manuf Technol 90:1457–1463. https://doi.org/10.1007/s00170-016-9333-6
15. Baran I, Cinar K, Ersoy N et al (2017) A review on the mechanical modeling of composite manufacturing processes. Arch Comput Methods Eng 24:365–395. https://doi.org/10.1007/s11831-016-9167-2
16. Toll S (1998) Packing mechanics of fiber reinforcements. Polym Eng Sci 38:1337–1350. https://doi.org/10.1002/pen.10304
17. Hwang JD, Lin HJ, Hwang WS et al (1995) Numerical simulation of metal flow and heat transfer during twin roll strip casting. ISIJ Int 35:170–177. https://doi.org/10.2355/isijinternational.35.170
18. Stolbchenko M, Grydin O, Samsonenko A et al (2014) Numerical analysis of the twin-roll casting of thin aluminium-steel clad strips. Forsch Ing 78:121–130. https://doi.org/10.1007/s10010-014-0182-x
19. Hesselbach J, Behrens B-A, Dietrich F et al (2007) Flexible forming with hexapods. Prod Eng Res Devel 1:429–436. https://doi.org/10.1007/s11740-007-0063-3
20. Dietrich F (2014) Non-linear modelling of hydraulically actuated production machines using optimised experiments. Schriftenreihe des Instituts für Werkzeugmaschinen und Fertigungstechnik der Technischen Universität Braunschweig. Vulkan, Essen, [München]
21. Behrens B-A, Bohne F, Lorenz R et al (2020) Numerical and experimental investigation of GMT compression molding and fiber displacement of UD-tape inserts. Procedia Manuf 47:11–16. https://doi.org/10.1016/j.promfg.2020.04.109
22. Zhang J, Wang J, Lin J et al (2016) Multiobjective optimization of injection molding process parameters based on Opt LHD, EBFNN, and MOPSO. Int J Adv Manuf Technol 85:2857–2872. https://doi.org/10.1007/s00170-015-8100-4